Proceedings of the Canadian Society for Mechanical Engineering International Congress
32nd Annual Conference of the Computational Fluid Dynamics Society of Canada
Canadian Society of Rheology Symposium
CSME-CFDSC-CSR 2025
May 25–28, 2025, Montréal, Québec, Canada

FINITE ELEMENT MODELLING OF A NON-PNEUMATIC TIRE'S SPOKE

William Collings[1*], Jackson Schwarz[2], Charles E. Bakis[2], Zeinab El-Sayegh[1], Moustafa El-Gindy[1]
[1]Department of Automotive and Mechatronics Engineering, Ontario Tech University, Oshawa, Canada
[2]Department of Engineering Science and Mechanics, Pennsylvania State University, University Park, United States
*william.collings@ontariotechu.ca

Abstract—In order to understand and design modern non-pneumatic tires (NPTs), it is important to characterize the stress-strain behaviour of the polyurethane rubber their spokes are often composed of. This study focuses on a particular under-studied type of NPT, a Michelin Tweel® 18x8.5N10 tire designed for use with golf and utility carts. Characterization of the polyurethane spoke material was done by calibrating three material models with an experimental stress-strain curve, and then validating the models with a simulated tensile test. Two different software packages, MCalibration and Pam-Crash, were used to calibrate a 3rd-order Ogden hyperelastic rubber model, and the resulting models had a high R^2 fitness of 0.99 with respect to the experimental data up to 500% strain. However, both Ogden models underestimated the stress in the range of 0% to 70% strain, therefore the General Nonlinear Solid Foam material model was implemented instead in order to exactly predict the polyurethane's stress-strain behaviour in the 0% to 70% strain range. This difference in accuracy over a specific range demonstrates the importance of considering a large number of material models in order to obtain the best performance in the desired range, rather than relying on fitness coefficients. The implementation of the General Nonlinear Solid Foam model for the polyurethane rubber will allow highly accurate modelling of the NPT spoke's behaviour in future finite element modelling endeavours.

Keywords-non-pneumatic tire; finite element analysis; Ogden model; tensile test

I. INTRODUCTION

Present developments in tire technology include the design of airless or non-pneumatic tires (NPTs), such as Michelin's line of Tweel® products [1] (Fig. 1). Optimization of these tire designs requires detailed knowledge of the rubber materials making up the different parts of the tire, in order to predict their behaviour under various operating conditions. A key step in the NPT design process is thus the characterization of material properties for material modelling in Finite Element Analysis (FEA). There are three major parts to this material modelling process: selecting a mathematic material model, experimentally measuring the material's properties and behaviour, and finally, validating the model.

The rubber compound used in the Michelin Tweel® spokes is a type of polyurethane [2], [3], with various additives blended in to achieve the desired stiffness and viscoelastic properties. The development of material models for such nonlinear elastic materials can be traced to the work of Treloar [4] and Rivlin [5]. Over time, different formulations based on strain energy conservation with varying numbers of parameters and complexity were proposed, such as the Neo-Hookean, Yeoh, Mooney-Rivlin, Arruda-Boyce, van der Waals, and Ogden models [6], [7]. Currently, the 3rd-order Ogden model is one of the more popular hyperelastic rubber models due to its flexibility and ability to incorporate experimental data for deformation modes other than uniaxial tension. The Ogden model was first proposed in 1972, and has since undergone many refinements and variations [8], [9]. An example of the Ogden model is shown in (1) [10]:

$$W = \sum_{A=1}^{3} \sum_{i=1}^{N} 2\frac{\mu_i}{\alpha_i}\left(\bar{\lambda}_A^{\alpha_i} - 1\right) + \frac{K}{2}(J-1)^2 \tag{1}$$

where N is the number of terms in the Ogden model, A is the index (1, 2, or 3) of the principle stretches $\bar{\lambda}_A$, W is the strain energy, K is the bulk modulus, J is the total volume ratio, and $\mu_{1\text{-}3}$ and $\alpha_{1\text{-}3}$ are the unknown Ogden coefficients. The second term is considered negligible for incompressible materials since J =1. Both K and $\mu_{1\text{-}3}$ carry the same units of stress, which are equivalent to energy, while the other parameters are dimensionless.

Figure 1. Example of an NPT, specifically a Michelin Tweel® 18x8.5N10 for golf carts.

The next step after a selecting a material model is performing experiments to characterize the material's mechanical behaviour, such as a uniaxial tensile or compressive test, biaxial tensile test, shear test, fatigue test, temperature test, or any other appropriate test [11], [12], [13]. The exact tests performed are chosen depending on the requirements of the material model, the operating conditions of the material, and the available test equipment. A density measurement is also required in order to use the material in a finite element model. For example, the full 3rd-order Ogden rubber model requires 3 datasets: uniaxial tension, biaxial tension, and shear [10]. However, if the component is known to undergo compression as part of its operating conditions, then compression tests should be included in the experimental dataset, and other tests such as shear may be omitted, because the goal of the material modelling is to predict its behaviour during the operating conditions.

Other researchers have specifically applied these material modelling methods to NPT spokes. Rugsaj and colleagues [14], [15] have been particularly active in this regard. In one instance [14], they used a novel inverse method to determine the modulus of elasticity of the spoke material. Both the physical NPT spoke and a virtual FEA model were subjected to the same 3-point bending test, and the modulus of elasticity in the FEA model was optimized to match the simulated and experimental loads. In another instance [15], they used ASTM D412 and D575 test standards to determine the tensile and compressive properties of the NPT spoke and tread rubbers in the course of developing an FEA model. Finally, a different group of researchers performed validation of a full-size NPT FEA model by comparing physical and simulated vertical stiffness and contact patch tests [16]. A key step was measuring the simulated spoke deflection to ensure it captured the behaviour of the physical tire.

One major difference between these previous studies and the present work is the type of NPT analyzed. The previous studies cited here all experimented on the Michelin Tweel® SSL line of heavy-duty NPTs, which have a different construction and use case than the Michelin Tweel® Turf NPTs for golf and utility carts [1], which are the focus of the present work, and have not been studied before to the authors' knowledge.

An important step in creating an FEA simulation based on the calibrated material models is verifying that the final model does in fact behave as expected. This can be done by validating the performance of the whole tire model against experiments [15], [16], or by directly simulating the compressive or tensile tests used to calibrate the material models [15], [17], [18]. In [15], high R^2 fitness coefficients were indicative of a material model that fit the experimental data well. Additionally, FEA simulations can be used to optimize the geometry of the specimens in the stress-strain tests [17], and to aid measurement of hard-to-measure quantities such as the true strain of steel under tension [18].

The present study adds to previous research by performing experimental work on a different kind of NPT for golf and utility carts, as well as using a different material model for the rubber behaviour. First, the material modelling and validation procedure will be described, followed by the results of the tensile test simulations, and then the conclusions.

II. Methodology

In this study, a material model was fit to the experimental stress-strain curve for an NPT spoke specimen using several different approaches. The tensile test procedure for obtaining the stress-strain curves was described in detail in [19]. Essentially, standard-size Type C specimens based on ASTM D412 [20] were subjected to cyclic tensile tests up to 500% strain. The results were averaged between two different test runs, and the averaged curves are shown in Fig. 2.

Only the first loading cycle was extracted from Fig. 2 to serve as the target for fitting the material model; the later cycles could be incorporated in the future via a separate hysteresis sub-model. The extracted curve consisted of 1000 engineering stress-strain datapoints. Next, a material model needed to be selected, in this case the 3rd-order Ogden rubber model [8], [9], [10]. The Ogden coefficients were determined with both the specialized curve-fitting software MCalibration [21], and the curve-fitter for the Ogden rubber model built into Pam-Crash 2023 which uses a nonlinear least squares method [10].

An important part of developing such a material model is validating it to ensure the predicted behaviour is as expected. In order to do the validation, a virtual tensile test was conducted, using an FEA model of the ASTM D412 Type C specimen in Pam-Crash. Initially, a full model of the specimen was created, with 22400 solid hexahedral elements (Fig. 3a), but then, due to the symmetry of the specimen, the model was reduced in size to only an eighth, with 2800 hexahedral elements (Fig. 3b). This is a typical practice for these types of simulated tests [17], [18], and it is advantageous because the much lower number of nodes and elements required allows the simulations to be run faster. The correctness of the reduced model can be seen by the identical Von Mises stress distribution, and the maximum Von Mises stress of 5.262 MPa which is identical to the full model and occurs at the same location. The size of the hexahedral elements was also varied, with the smallest elements (0.516 mm by 0.375 mm by 0.275 mm) being used in the narrow gauge section and the largest (1.549 mm by 1.563 mm by 0.275 mm) at the grip ends. The overall size of the full model was 115 mm by 25 mm by 2.75 mm, with the eighth model having all of the dimensions reduced by half. Note that in an attempt to run stable simulations of the tensile test up to 500% strain, the initial FEA model was modified by halving the element size in the x-direction, consequently doubling the number of elements and reducing the distance each element needed to stretch.

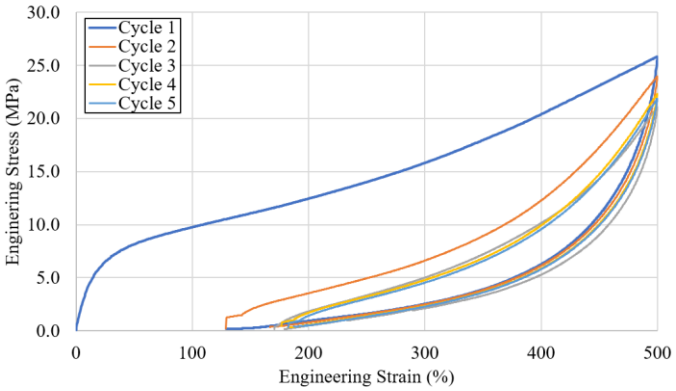

Figure 2. 5 cycles of engineering stress-strain for Type C NPT spoke specimen (modified from [19]).

The boundary conditions for the model (Fig. 4) included global gravitational acceleration and damping, a fixed constraint on the wide end of the specimen where the grip would be, as well as on the planes of symmetry, and finally an imposed velocity condition (V_x) on the narrow or neck end of the specimen, equal to 0.5 mm/s, or half the nominal extension rate of 60 mm/min. The coordinates of key nodes at the neck end of the specimen were tracked in order to precisely record the changes in length and cross-section of the specimen, as well as the section force at the neck end. Finally, the engineering stress and strain were recalculated and compared to the experimental curve for validation.

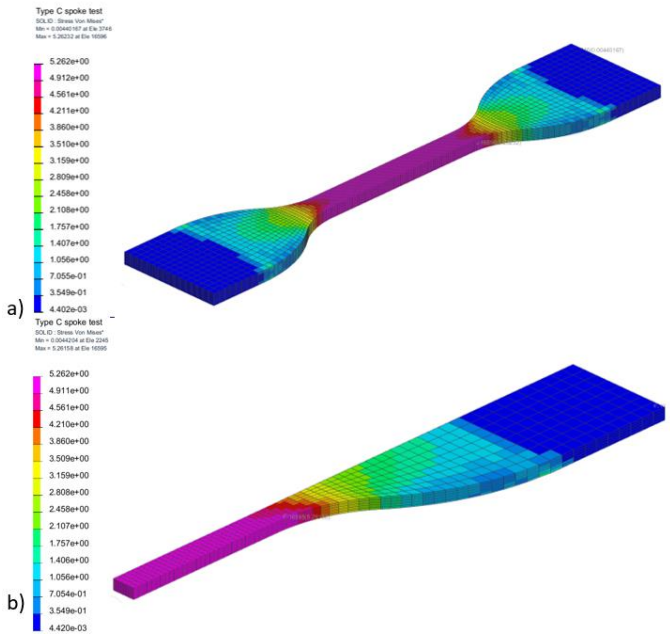

Figure 3. a) full specimen model, b) eighth specimen model. The color scale on the left shows the Von Mises stress in MPa.

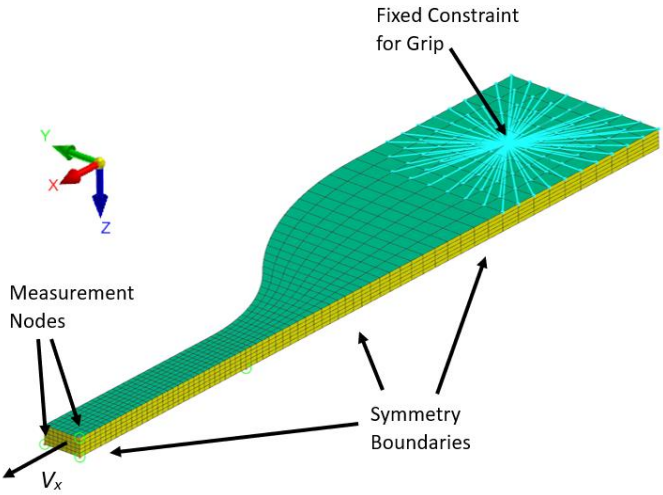

Figure 4. Boundary conditions and measurement nodes for eighth specimen FEA model. The symmetry boundaries are highlighted in yellow, and also include the underside.

III. Results and Validation

First, the Ogden rubber model was calibrated using the dedicated MCalibration software for curve-fitting material models. In Fig. 5, it can be seen that the results were very good for a 3rd-order Ogden model, with an R^2 fitness of 0.99. The fit is nearly perfect in the range of 100% to 450% strain, however, there is some deviation between 450% to 500% strain, and the predicted stress is substantially lower in the 0% to 100% strain range. Unfortunately, the MCalibration software calculated the coefficients specifically for the LS-DYNA form of the Ogden rubber model, and the coefficients did not produce the expected results when copied into Pam-Crash. Thus, a different calibration method was required.

Next, the same task was done using the curve-fitter built into Pam-Crash, which produced good results, with an overall R^2 fitness of 0.99 (Fig. 6). However, the fitted curve showed a small amount of deviation between 100% to 200% strain, and predicted substantially lower stresses from 0% to 70% strain. This last difference is a significant problem with the model, since the NPT spokes undergo only small strains, on the order of 2% [16]. Hence, it was necessary to find a different material model capable of accurately predicting the stress-strain curve at less than 70% strain.

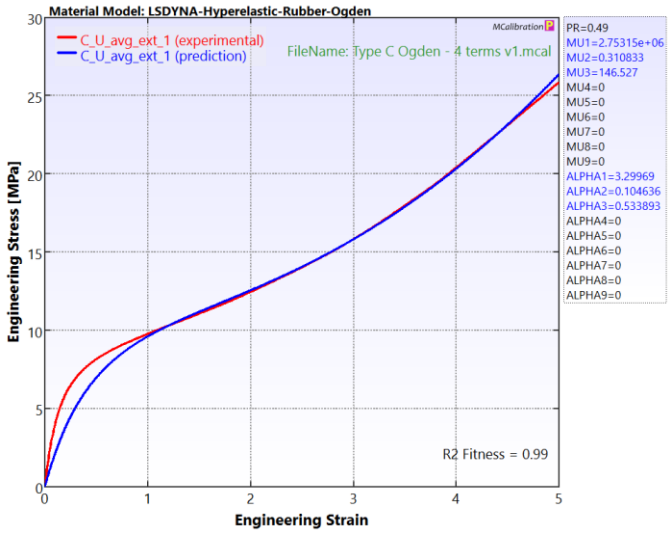

Figure 5. MCalibration results for 3rd-order Ogden model from 0 to 500% strain.

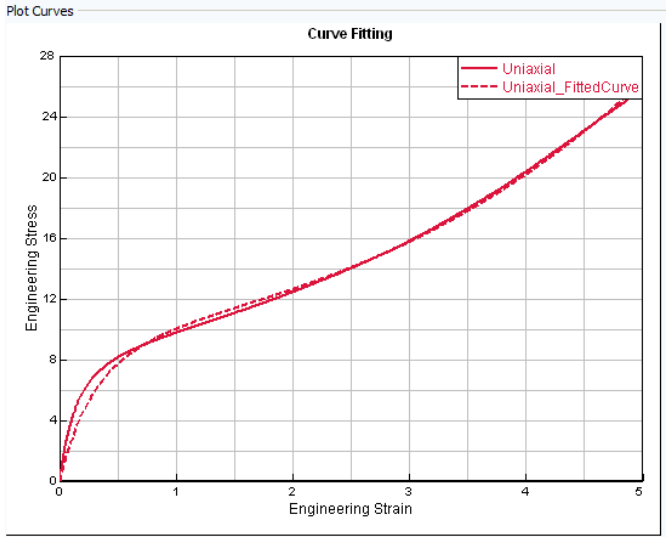

Figure 6. Calibration results for 3rd-order Ogden model using the Pam-Crash curve-fitter from 0 to 500% strain.

Table 1 shows the difference in the calibrated Ogden coefficients from the two different curve-fitters. Notice how Pam-Crash found a solution with negative coefficients, and the large order of magnitude difference in some of the MCalibration coefficients. These differences are due not only to the mathematical differences between the Pam-Crash and LS-DYNA versions of the Ogden model, but also due to the under-determination of the 3rd-order Ogden coefficients when calibrating against a single uniaxial tension curve. It is possible for the same algorithm to determine different sets of coefficients that fit the model to the same experimental data [9].

TABLE I. CALIBRATED 3RD-ORDER OGDEN MODEL COEFFICIENTS

Ogden Coefficient	Curve-Fitting Software	
	MCalibration	*Pam-Crash*
μ_1[a]	2.75315×10^6	-2.4
μ_2[a]	0.310833	0.0621
μ_3[a]	146.527	-2.7
α_1	3.29969	-2.07
α_2	0.104636	3.7
α_3	0.533893	-2.07

a. μ coefficients carry units of MPa.

Since neither of the two curve-fitters produced models with high accuracy at the required low strains, a third approach needed to be taken. In this case, it was the Type 45 General Nonlinear Solid Foam model in the Pam-Crash material library [10]. This model took as input a series of compression and tension stress-strain curves at different strain rates, which meant the experimental stress-strain curve for the NPT spoke specimen could be used as a direct input. The same input curve was used for both the compression and tension curve inputs, and the initial Young's Modulus was estimated to be 47.77 MPa from the experimental stress-strain curves. The tensile curve was duplicated for the compression curve input based on the assumptions that the effect of the compressive behaviour on a simulated tensile test would be negligible, and that the compressive behaviour would be similar to the tensile behaviour for the small strains experienced by the NPT spokes. The dashed line in Fig. 7 shows the predictions of the General Nonlinear Solid Foam model, which exactly match the experimental data at low strains, unlike the calibrated Ogden model. However, there is a clear discrepancy with the General Nonlinear Foam model starting at approximately 350% strain. This is due to the challenges involved in simulating large strains with FEA. For example, obtaining the curve in Fig. 7 required halving the element size from the initial model in order for the time step to remain stable. The Ogden model curve in Fig. 7 does not suffer from these limitations since it came directly from the calibrated curve in Fig. 6.

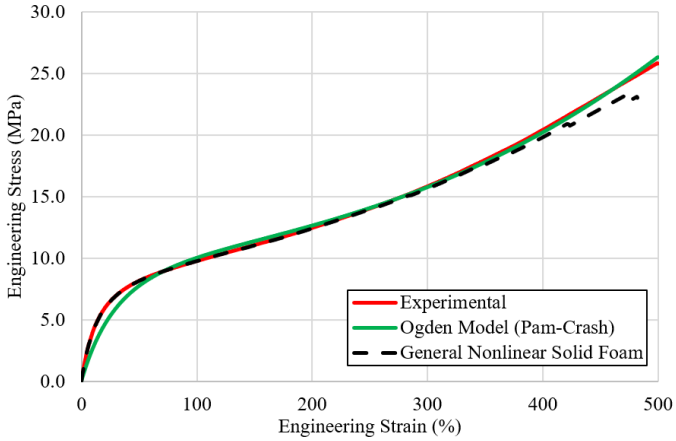

Figure 7. Comparison of General Nonlinear Foam model to Ogden model and experimental stress-strain curve from 0% to 500% strain.

These results demonstrate the importance of attempting to use as many material models as possible in order to find one that provides accurate material behaviour predictions in the desired range. The 3rd-order Ogden model is a sophisticated hyperelastic material model with 6 coefficients, which was calibrated to a very high degree of fitness to match the experimental data. However, it was still unable to provide accurate predictions at low strains. This is partly due to the way the Ogden model was design for high-strain hyperelastic materials, but it still underscores the importance of properly validating a material model rather than relying on high fitness values for the calibrated coefficients.

IV. CONCLUSIONS

In this study, previously obtained stress-strain data from a uniaxial tension test was used to calibrate several material models with the goal of accurately predicting the first cycle behaviour of the polyurethane rubber used in an NPT spoke. The experimental data used for calibration consisted of a single extension stroke from 0% to 500% strain. Three different material modelling approaches were applied: calibrating a 3rd-order Ogden rubber model using the curve-fitters from the MCalibration and Pam-Crash software packages; and then using a different General Nonlinear Solid Foam material model for better accuracy in the low-strain region between 0% to 70%. The modelling methods were validated with a simulated FEA tensile test. It was discovered that both curve-fitters were able to calibrate the Ogden models to the experimental data with a high degree of accuracy (R^2 of 0.99). However, despite having an impressive R^2 fitness for the entire strain range of 0% to 500%, there was a substantial underestimation of the experimental stress for both Ogden models in the low-strain region of 0% to 70%. Hence, the General Nonlinear Solid Foam material model was applied which was able to replicate the experimental results in that range exactly. This deficiency in well-calibrated material models demonstrates the importance of searching for the best model for task at hand, rather than trusting in the most popular model without doing proper validation. With accurate material models for the full range of strains from 0% to 500%, the polyurethane spoke material is ready to be incorporated into a full NPT FEA model. Future work will also include developing a hysteresis sub-model to predict the behaviour of the polyurethane over multiple loading cycles.

REFERENCES

[1] Michelin North America, “Michelin Tweel family brochure,” 2022. Available: https://tweel.michelinman.com/on/demandware.static/-/Sites-tweel-us-Library/default/dw9dbd0fd8/pdf/Michelin_Tweel_Full_Line_Brochure.pdf.

[2] Rehabilitation Engineering Research Center on Technology Transfer, "Michelin Tweels technology/value description," State University of New York at Buffalo, Buffalo, New York, October 2005. Available: https://publichealth.buffalo.edu/content/dam/sphhp/cat/kt4tt/pdf/leahy/Michelin%20Tweels%20Comm%20Pkg.pdf.

[3] A. Parfondry, M. E. Dotson, C. B. Clayton, and A. Delfino, "Polyurethane support for non-pneumatic tire," European Patent 3 071 424 B1, May 26, 2021. Available: https://patents.google.com/patent/EP3071424B1/en?q=(~patent%2fUS5223599A).

[4] L. R. G. Treloar, "Stress-strain data for vulcanised rubber under various types of deformation," Trans. Faraday Soc., vol. 40, pp. 59–70, 1944, doi:10.1039/TF9444000059.

[5] M. Destrade, J. Murphy, and G. Saccomandi, "Rivlin's legacy in continuum mechanics and applied mathematics," Phil. Trans. Royal Soc. A: Mathematical, Physical and Engineering Sciences, vol. 377, no. 2144, pp. 20190090, March 2019, doi:10.1098/rsta.2019.0090.

[6] G. Anghelache and R. Moisescu, “Analysis of rubber elastic behaviour and its influence on modal properties,” Materiale Plastice, vol. 45, no. 2, pp. 143-148, June 2008.

[7] P.-S. Lin, O. Le Roux de Bretagne, M. Grasso, J. Brighton, C. StLeger-Harris, and O. Carless, “Comparative analysis of various hyperelastic models and element types for finite element analysis,” Designs, vol. 7, no. 6, pp. 135, November 2023, doi:10.3390/designs7060135.

[8] R. W. Ogden, "Large deformation isotropic elasticity – on the correlation of theory and experiment for incompressible rubberlike solids," Proc. Royal Soc. London: A. Mathematical and Physical Sciences, vol. 326, no. 1567, pp. 565-584, February 1972, doi:10.1098/rspa.1972.0026.

[9] M. Destrade, L. Dorfmann, and G. Saccomandi, "The Ogden model of rubber mechanics: 50 years of impact on nonlinear elasticity," Phil. Trans. Royal Soc. London: A. Mathematical, Physical and Engineering Sciences, vol. 380, no. 2234, pp. 20210332, October 2022, doi:10.1098/rsta.2021.0332.

[10] Y. Yamashita, H. Uematsu, and S. Tanoue, “Calculation of strain energy density function using Ogden model and Mooney–Rivlin model based on biaxial elongation experiments of silicone rubber,” Polymers, vol. 15, no. 10, pp. 2266, doi:10.3390/polym15102266.

[11] M. A. Tapia-Romero, M. Dehonor-Gomez, L. E. Lugo-Uribe, "Prony series calculation for viscoelastic behavior modeling of structural adhesives from DMA data.", Engineering Research and Technology (Mexico), vol. 21, no. 2, pp. 1-10, April 2020, doi: 10.22201/fi.25940732e.2020.21n2.014.

[12] A. Tcharkhtchi, S. Farzaneh, S. Abdallah-Elhirtsi, B. Esmaeillou, F. Nony, and A. Baron, "Thermal aging effect on mechanical properties of polyurethane," Int. J. Polymer Analysis and Characterization, vol. 19, no. 7, pp. 571-584, October 2014, doi: 10.1080/1023666x.2014.932644.

[13] ESI Group. (2023). Virtual Performance Solution 2023: Solver Reference Manual.

[14] R. Rugsaj and C. Suvanjumrat, "Determination of material property for non-pneumatic tire spokes by inverse method," Key Engineering Materials, vol. 777, pp. 411-415, August 2018, doi: 10.4028/www.scientific.net/KEM.777.411.

[15] R. Rugsaj and C. Suvanjumrat, "Proper radial spokes of non-pneumatic tire for vertical load supporting by finite element analysis," Int. J. Automotive Technology, vol. 20, no. 4, pp. 801-812, Aug 2019, doi: 10.1007/s12239-019-0075-y.

[16] M. Żmuda, J. Jackowski, and Z. Hryciów, "Numerical research of selected features of the non-pneumatic tire," in Computational Technologies in Engineering (TKI’2018), Jora Weilka, Poland, October 16-19, 2018, vol. 2078, no. 1, pp. 020027-1 to 020027-8, doi: 10.1063/1.5092030.

[17] Y. Hanabusa, H. Takizawa, and T. Kuwabara, "Numerical verification of a biaxial tensile test method using a cruciform specimen," J. Materials Processing Technology, vol. 213, no. 6, pp. 961-970, June 2013, doi: 10.1016/j.jmatprotec.2012.12.007.

[18] H. D. Kweon, J. W. Kim, O. Song, and D. Oh, "Determination of true stress-strain curve of type 304 and 316 stainless steels using a typical tensile test and finite element analysis," Nuclear Engineering and Technology, vol. 53, no. 2, pp. 647-656, February 2021, doi: 10.1016/j.net.2020.07.014.

[19] W. Collings, C. Li., J. Schwarz, A. Lakhtakia, C. Bakis, Z. El-Sayegh, and M. El-Gindy, “Mechanical analysis of a non-pneumatic tire’s spokes,” 25M-0031, SAE World Congress Experience, April 8-10, 2025, Detroit, USA, in press.

[20] ASTM International, “Standard test methods for vulcanized rubber and thermoplastic elastomers—tension,” ASTM D412-06, December 2006.

[21] ANSYS, “MCalibration: advanced polymer and material calibration software,” 2025. Available: https://www.ansys.com/products/structures/mcalibration.